

## Percolation threshold and scattering power law of gelatin gels

Y. Piñeiro,<sup>1</sup> M. A. López-Quintela,<sup>2</sup> J. Rivas,<sup>1</sup> and D. Leisner<sup>2</sup><sup>1</sup>Department of Applied Physics, University of Santiago de Compostela, Campus Sur, E-15782 Santiago de Compostela, Spain<sup>2</sup>Department of Chemistry Physics, University of Santiago de Compostela, Campus Sur, E-15782 Santiago de Compostela, Spain

(Received 27 June 2008; revised manuscript received 22 January 2009; published 29 April 2009)

Gelation of gelatin was broadly studied by experimental and theoretical methods. Power laws observed on the gel point—mainly obtained by dynamic light scattering (DLS)—are considered to be the signature of some special dynamic phenomena ascribed to the appearance of a percolation cluster. We present here experimental (DLS and rheometric measurements) and Monte Carlo simulation studies showing that the percolation threshold and DLS power-law decay occur on different times. We ascribe the percolation point to the time where the scattering medium mode diverges. This mode is sensitive to the clusters' growth and diverges when the system attains the percolation threshold. The power-law behavior is obtained only in the postpercolation regime.

DOI: 10.1103/PhysRevE.79.041409

PACS number(s): 82.70.Gg, 82.35.Lr

Gelatin is a linear biopolymer obtained from denatured collagen. Gelatin-water systems undergo gelification at room temperature by forming reversible hydrogen-bonded triple helices. This aggregation process transforms the liquid solution into a macroscopic viscoelastic network, and the gel point is usually determined by experimental criteria as  $G' \propto G'' \propto \omega^n$  [1] or  $S(q, t) \propto t^{-\varphi}$  [2]. The percolation approach [3] has become the most used theoretical frame for predicting the physical properties of the gel and the gel point. It describes a gelation process through the gradual increase in links between particles of small length  $n$ , and the state of the network is expressed in terms of the fraction  $p$  of created links. For small  $p$  only isolated clusters exist. However above a threshold value  $p=p_c$ , clusters become interconnected and form a spanning network, which defines the sol-gel transition. On  $p_c$  power-law behavior is expected for static properties, the size distribution of clusters,  $n(m) \propto m^{-2.18}$ , or the typical cluster radius (correlation length)  $\xi \propto (1-p/p_c)^{-0.88}$ , and, for the experimentally more obvious, macroscopic elastohydromechanical properties such as the equilibrium modulus  $G'_0 \propto (1-p/p_c)^b$  and zero-shear viscosity  $\eta \propto (1-p/p_c)^{-k}$  [4].

For chemical gels the percolation threshold coincides with and describes the experimental gel point, although many theoretical refinements including precise accounting of cyclization effects have been done to achieve a precise description of the gel point [5]. However, a different situation has been reported in colloidal aggregation systems [6,7], in reversible tetrafunctional monomers undergoing gelation [8], or in the bonding process between oil droplets and telechelic polymers [9], where percolation and gelation seem not to occur simultaneously. In the specific case analyzed in the present work, long biopolymers undergoing physical gelation, various reasons can be envisaged for this distinguishable behavior.

On one hand, the basic building units of the gelatin linking process are long chains ( $n > 1$ ), substantially different from the small length units of the percolation approach. In fact, the chain length separates the two possible universality classes that may explain gelation [10]: (bond or site) percolation (very small  $n$ ) and vulcanization (the cross-linking of very large chains  $n \gg 1$ ) which in certain semidilute [11] and melt [12] conditions recover some of the percolation predic-

tions. Gelatin gelation, with an intermediate value of  $n$ , will exhibit crossover behavior between both and accordingly the universal exponents may be different.

In addition, percolation models are static and irreversible, while real polymers have mobility and may aggregate reversibly. Indeed, computer simulation studies [13] on kinetic gelation have shown that varying the reversibility probability  $r$  in the range of  $r=[0.0, 0.5]$  has a strong influence on the critical exponents of the correlation length  $\nu=[0.95, 0.75]$  and the gel fraction  $\beta=[0.37, 0.65]$ , while the cluster-size distribution exponent  $\tau=[2.16, 2.31]$  remains steady. Also, experimental measurements done with gelatin gels [14] show variations in  $b=[2.45, 1.64]$  and  $k=[2.6, 1.1]$  depending on the temperature quench  $T_Q$  and the concentration  $\Phi$  of the system.

Finally, the mapping of  $p$ , the bond percolation probability, unto time  $t$ , temperature  $T$ , or concentrations  $\Phi$  axis, is being lately under reexamination [15] due to its consequences on the relations that held on the critical region.

For a gelatin gel, although the bond fraction  $p$  is equivalent to the normalized helices' (links of the network) amount  $\psi$  (number of helices on each temperature divided by the total possible helices amount) [16],  $p \approx \psi$ , the mapping unto the time  $t$  is related to the specific process that causes the formation of a link. It has been reported that  $\psi$  presents two kinetic processes [17], from which the rapid one follows an exponential function:  $\psi(t, T_Q) = \psi(T_Q)[1 - \exp(-t/t_f)]$ . For a certain quenching temperature, the parameter  $\psi(T_Q)$  remains constant during gelation, and only  $\chi(t) = [1 - \exp(-t/t_f)]$  retains the steep increase in the helices' amount in the critical region  $\zeta = (1-p/p_c)$ . Introducing  $\chi(t)$  as the correct time mapping of  $p$  for gelatin gelation into the zero-shear viscosity relation, one obtains now

$$\eta \propto (1-p/p_c)^{-k} \propto \exp[k(t/t_f)], \quad (1)$$

i.e., an exponential time dependence, which has been already taken as the percolation threshold signature for collagen gelation [16].

Among the techniques used to monitor percolation and gelation, rheology, on the limit of minimum shear, and dynamic light scattering (DLS), in the limit of minimal thermal lensing, are the most prominent.

DLS techniques probe the relaxation of density fluctuations of momentum transfer  $q$  through the evolution of the normalized intensity correlation function  $I(q,t)$ , which is connected to the dynamic structure factor  $S(q,t)$  through a general relation [18]. By obtaining the time relaxation spectra of  $S(q,t)$ , valuable microscopic information about length scales and their associated dynamics has been determined for polymer-solvent systems [19,20]. It is used to investigate the structural complexity of gelatin gelation, in which clusters of different sizes, diffusing through the solution of nonaggregated and diffusing chains, in addition to interjunction flexible segments oscillating around an averaged position and junction points with a very restricted mobility (that may eventually unbind giving rise to very slow structural readjustments of the network), contribute to three dynamic modes.

These modes have been a source of controversy. In previous works, we have provided a possible comprehensive explanation [21] by carefully studying dependences on concentration, temperature, and scattering vector, and successfully used it to study the complex interplay of gelation and microphase separation of gelatin-maltodextrin mixtures [22].

In this paper we present experimental and numerical results showing that for a semidilute gelatin solution, the percolation threshold is attained first by the system, and only afterward is the more hindered dynamically gel point attained.

We have analyzed gelatin solutions in a range of concentrations and temperature quenches wider than those in other papers [2,23,24], covering from dilute to semidilute conditions,  $\Phi=[1,7.5]\%$  (w/w) and fast and slow gelation  $T_Q=[15,30]$  °C. Alkaline-processed lime hide gelatin (LH1e: 240 Bloom, pI 4.7,  $M_n=83.3$  kD,  $M_w=146$  kD) was solved in filtered solution of salt in bidistilled water with 0.05% (w/w) of sodium azide, and 0.1M sodium chloride resulting in a pH=[6,7]. After swelling at 45 °C and 0.5 h stirring gently at 60 °C, the solution was filtered through 0.45  $\mu\text{m}$  porous cellulose.

Dynamic light scattering was performed using a right-angle ALV SP-86 goniometer equipped with a photomultiplier tube (PMT) detector. A vertically polarized laser beam (Spectra Physics 127 helium-neon laser, 60 mW, wavelength  $\lambda_0=632.8$  nm), was focused to the sample vat. Far-field intensity correlation functions  $g_2(t \equiv \text{lag time})$  were recorded for a momentum transfer  $q=18.7 \mu\text{m}^{-1}$  and their time correlation analyzed by an ALV-5000 multiple-tau correlator. The data were analyzed in terms of the electric field autocorrelation function  $g_1(t)=[g_2(t)-1]^{0.5}=\int A(\tau)\exp(-t/\tau)d \ln \tau$  by the CONTIN algorithm, in order to obtain the relaxation time spectra  $A(\tau)$  as their inverse Laplace transforms in the  $\tau$  range from 1  $\mu\text{s}$  up to 10<sup>3</sup>s on logarithmic scale. Assuming homodyne light beating, and applying the relation  $D=1/(q^2\tau)$ , and the Stokes-Einstein relation  $D=k_B T/6\pi\eta\xi$ , where the local viscosity  $\eta$  is approximated by the solvent (brine) viscosity  $\eta_0$ , then the  $\tau$  data were transformed to diffusivities ( $D$ ) or apparent correlation lengths ( $\xi_{app}$ ).

Rheometric analysis was done by pouring the hot solutions into a thermostated ( $\pm 0.1$  °C) cold stainless-steel stator of the SSA21 adapter of a Brookfield DV2+ viscometer. Immediately (at  $t_{set}=0$  s) the filled stator was lifted so that

the cold rotor dived in. The 2 mm gap allowed a complete cooling on 20 s. Operating on medium speed of rotation, the applied shear rate was 9.3 Hz, and the stress was less than 0.75 N m<sup>-2</sup> before gelation occurred. The start of the first linear viscosity increase (up to several Pa s) was taken as the viscosity gel time  $t'_{gel}$ .

In addition we [25] have applied a dynamic Monte Carlo (MC) method to a cubic lattice, to model reversible associating polymers in solution, which mimic the triple-helix aggregation mechanism proposed to rule for gelatin [26]. It is based on a dynamic algorithm previously employed to study linear polymer solutions [27] that produces sol configurations with the expected polymeric static and dynamic properties under different thermal conditions, different from random walk (RW) configurations obtained by a simple percolative scheme.

We have simulated  $N$  monodisperse polymer chains, with lengths in the range of  $n=[36,100]$ , on a cubic lattice with boundary conditions in all directions. A fraction of associative slabs,  $\Phi_c$ , has been randomly placed over the nonassociative chains. Thermal behavior is defined by the attractive interaction energy  $\varepsilon/k_B T$  between nearest neighboring nonassociative slabs. Gelation is defined by a high attractive interaction term,  $\varepsilon_h/k_B T$ , that binds three nearest neighboring associative slabs. Only associative slabs coming from three different chains are allowed to become a triple-helix junction point as it is supposed to happen in the triple-helix gelatin aggregation [26]. The ratio  $R=\varepsilon_h/\varepsilon$  is a measure of the reversibility of the gel. All slabs move according to a predefined set of local jumps [28] that produces the Metropolis-biased configurational relaxation of the whole system and also of the junction point slabs, without unbinding them, giving rise to a more realistic relaxation of the network [29].

The thermal quenching has been implemented by increasing the interaction energy (equivalent to reduce the temperature) every  $[10^6, 5 \times 10^6]$  cycles per slab.

To avoid shearing perturbation we present only the rheology and scattering data for semidiluted gelatin solution,  $\Phi=5\%$  (w/w), and quenched from 60 to 22.5 °C, well below the gelation temperature.

In Fig. 1, the DLS correlation length spectra of the sample gelation can be observed in which f, m, and s correspond, respectively [21], to fast, (collective diffusion of “blobs” through the solution), medium (microheterogeneities, or anomalous self-diffusion of clusters [20]), and slow (finite “lifetime” of the transient network) modes whose intensity is given by the darkness of the shading. It can be observed that the medium mode increases very sharply after an induction period, and then suddenly breaks into a slow component  $s'$  and a secondary less intense medium  $m'$  with a smaller correlation length,  $\xi_{m'} < \xi_m$ . This sharp physical event happens at a time  $t_{per}=5760$  s and the medium-scale length is the relevant parameter for describing the percolation transition as we will show below by comparison to the viscosity evolution.

For the same sample, in Fig. 2, the time evolution of  $g_1(q,t)$  for  $q=18.7 \mu\text{m}^{-1}$  at different reduced times is presented. The correlation function taken over an extended relaxation time domain shows an initial exponential followed by 4 decades of a power law on  $t_{per}=6700$  s (normalized to

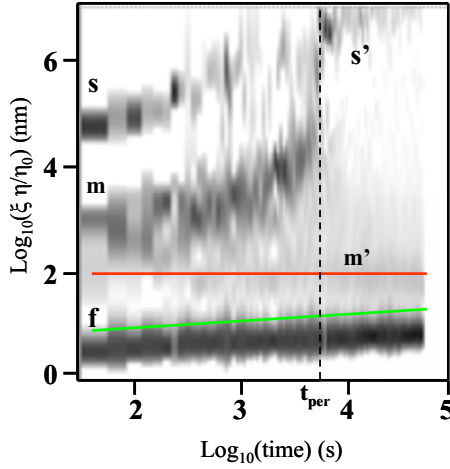


FIG. 1. (Color online) Time evolution of the correlation length spectra for a 5% LH1e gelatin quenched to 22.5 °C. The relative mode intensities are given by the darkness of the shading.

$t/t_{pl}=1$  in Fig. 2) and corresponds experimentally to the gel point [2]. It has to be observed that on  $t_{per}=5760$  s (corresponding to  $t_{per}/t_{pl}=0.85$  in Fig. 2), the breakup of the medium mode time presents a complete relaxation achieved by a combination of simple and stretched exponential decays and clearly precedes gelation (on  $t/t_{pl}=1$ ).

In Fig. 3, the normalized viscosity ( $\eta_0$  brine viscosity) and the apparent (or averaged) medium correlation length  $\xi_m$ , which describes the gelatin pregel clusters' growth, against the reduced time  $t_r=t/t_{per}$  are presented together.

A short induction period can be observed in zone I, where  $\xi_m$  increases steeply, while viscosity remains low and constant. The first triple-helical junctions begin to form and the system becomes a solution of gelatin chains with a few clusters.

Afterward  $\xi_m$  and  $\eta/\eta_0$  increase exponentially together with the same rate, zone II, as predicted by Eq. (2) to be the percolation threshold signature. During this period, the mean size of clusters grows until a maximum size is attained.

In zone III, the system is a solution of very large clusters, and the viscosity growth rate becomes steeper, while the medium mode splits into a slow mode  $s'$  (which converges with the former  $s$ ), and a secondary medium mode  $m'$  (less in-

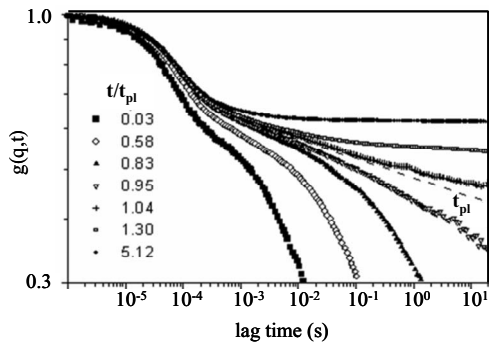


FIG. 2. Time evolution of the dynamic structure factor at different reduced times, below and above the gel point ( $0.03 < t/t_{pl} < 5.12$ ). Experimental conditions: same as in Fig. 1.

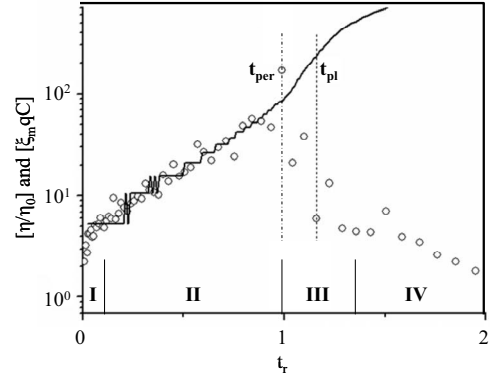


FIG. 3. Evolutions of the medium mode  $\xi_m$  (circles) and the reduced viscosity  $\eta/\eta_0$  (line) as functions of the reduced time  $t_r = t/t_{per}$ . Experimental conditions: same as in Fig. 1.

tense and with a smaller correlation length than the former  $m$ ; see Fig. 1). The gel network spans over the whole system and becomes steadily connected, so the slow structural relaxation is less probable (less intense  $s'$  mode). The clusters that remain free (split  $m'$  mode) are small ( $\xi_{m'} < \xi_m$ ) and become progressively attached to the network (the mode intensity disappears softly). This is the postpercolation regime. During this regime  $S(q, t)$  attains a power law, denoted by  $t_{pl}$  in the figure, clearly separated from  $t_{per}$ .

Finally in zone IV, the viscosity enters into a regime of smooth saturation and gelation is completed.

We ascribe the medium mode breakup time to the percolation threshold, and it clearly precedes the gelation point  $t_{pl}$ , dynamically more restricted with a high viscosity.

To verify these experimental results, MC simulations were carried out for different simulation conditions. For clarity, in what follows we will present only the results for a system of chains with length  $n=48$ , volume fraction  $\Phi=0.3$ , associative slabs fraction  $\Phi_c=0.3$ , and reversibility  $R=20$ .

We have directly measured the number of aggregates made up of  $m$  chains,  $n(m)$ , for each configuration and obtained the configurational average of this value at each temperature,

$$\langle n(m) \rangle = \frac{\sum_{i=1}^{n_{conf}} n(m)_i}{n_{conf}}, \quad (2)$$

and the dynamic structure factor  $S_{col}(q, \tau)$ , as usually referred for a lattice MC [30]:

$$S_{col}(q, \tau) = L^{-3} \left\langle \sum_{j=1}^{n_s} \sum_{k=1}^{n_s} f_j(t) f_k(t + \tau) \times \exp\{i\vec{q} \cdot [\vec{r}_j(t) - \vec{r}_k(t + \tau)]\} \right\rangle, \quad (3)$$

where  $\vec{r}_k$  are the lattice sites' positions, occupied by polymer or solvent, and  $f_k$  is the contrast factor, associated with the local refractive index of site  $k$ , given by  $f_{pol}=(1-\Phi)$  and

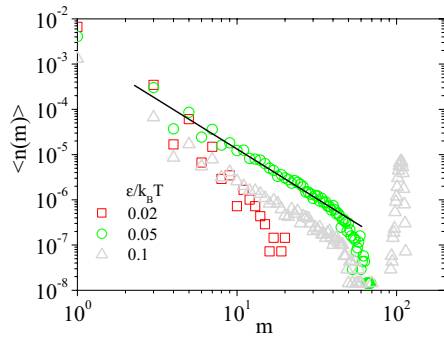


FIG. 4. (Color online) Cluster-size distribution evolution with reduced temperature (simulation conditions referred in the text). Linear fitting (straight line) gives an exponent  $\tau = -2.19 \pm 0.05$  on  $\epsilon/k_B T = 0.05$ , indicating percolation threshold.

$f_{\text{sol}} = -\Phi$ , and finite values of  $q$ ,  $q_n = (2\pi/L)n$ , with  $n = 1, 2, \dots, L$  for all space directions  $\{x, y, z\}$ .

In Fig. 4,  $\langle n(m) \rangle$  is presented against  $m$  for different reduced energies (inverse of temperature). In the sol phase,  $\epsilon/k_B T = 0.02$ ; only part of the chains are aggregated into clusters of small sizes. On  $\epsilon/k_B T = 0.05$  a large amount of chains is aggregated and the size distribution follows a power-law decay  $n(m) \propto m^{-2.19}$ , whose exponent is quite the same as the one predicted by percolation theory,  $\tau_{\text{per}} = 2.18$ , indicating that the percolation threshold has been reached. Afterward, on  $\epsilon/k_B T = 0.1$ , the asymmetric bimodal size distribution with a protuberance on the large-cluster region indicates that the postpercolation period is attained [31]. This result points directly to percolation as the gelatin universal class, rather than other models (diffusion limited cluster aggregation, kinetic arrest, jamming) that have been considered as possible candidates [32] to explain reversible aggregation processes.

In Fig. 5,  $f(q_1, \tau)$ , normalized values of the dynamic structure factor by  $S_{\text{col}}(q_1, 0)$ , for  $q_1 = (2\pi/L)$  is presented in double-logarithmic scale against MC time for the same system as in Fig. 4. In the sol phase,  $\epsilon/k_B T = 0.02$ ; the typical simple exponential decay of a solution is obtained. On the

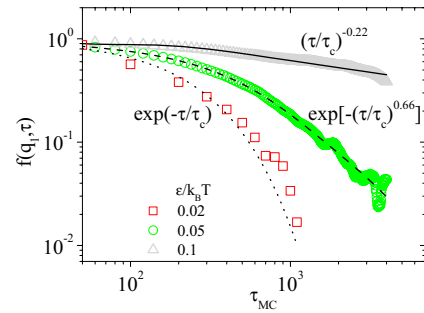


FIG. 5. (Color online) Dynamic structure factor against MC times for different reduced temperatures (simulation conditions: same as in Fig. 4). Only in the postpercolation threshold  $\epsilon/k_B T = 0.1$  is a clear power law attained with an exponent  $\varphi = -0.22$ , which is the experimental signature of gelation.

percolation point  $\epsilon/k_B T = 0.05$ , obtained from Fig. 4, the dynamics of the system is not significantly affected by the percolation transition since the decay of  $f(q_1, \tau)$  follows a stretched exponential,  $f(q_1, \tau) \propto \exp[-(\tau/\tau_c)^\beta]$ , with  $\beta = 0.66$ , in the range of some reported values [2],  $\beta = [0.65, 0.98]$  for gelatin gels. Therefore, the self-similar distribution of flexible clusters still retain dynamic degrees of freedom (by self-diffusion and local internodal segmental oscillations) and are able to relax on the scattering lengths. Only afterward, in the postpercolation region, when the three-dimensional network stays steadily connected,  $\epsilon/k_B T = 0.1$ , is a well-developed power-law decay attained,  $f(q_1, \tau) \propto (\tau/\tau_c)^\varphi$  with  $\varphi = -0.22$ . The value of  $\varphi$  depends on the simulation parameters, but remains always  $\varphi < 1$ . This agrees with the experimental results and allows concluding that, at least, in gelatin gels the hindered dynamically gel point is attained after percolation threshold. It should be interesting to explore if this is a general behavior for all biopolymer physical gels.

We want to acknowledge the financial support of the Concellería de Educación e Ordenación Universitaria (Xunta de Galicia, Spain) project “Grupos de Referencia Competitiva,” Project No. 2006/81.

- [1] F. Chambon and H. Winter, *J. Rheol.* **31**, 683 (1987).
- [2] S. Z. Ren, W. F. Shi, W. B. Zhang, and C. M. Sorensen, *Phys. Rev. A* **45**, 2416 (1992).
- [3] P. G. de Gennes, *Scaling Concepts in Polymer Physics* (Cornell University Press, Ithaca, 1988); D. Stauffer and A. Aharony, *Applications of Percolation Theory* (Taylor & Francis, London, 1992).
- [4] D. Stauffer, A. Coniglio, and M. Adam, *Adv. Polym. Sci.* **44**, 103 (1982).
- [5] K. Suematsu, *J. Phys. Soc. Jpn.* **75**, 064802 (2006).
- [6] E. Del Gado, A. Fierro, L. de Arcangelis, and A. Coniglio, *Phys. Rev. E* **69**, 051103 (2004).
- [7] M. C. Grant and W. B. Russel, *Phys. Rev. E* **47**, 2606 (1993).
- [8] A. Hasmy and R. Jullien, *Phys. Rev. E* **53**, 1789 (1996).
- [9] P. I. Hurtado, L. Berthier, and W. Kob, *Phys. Rev. Lett.* **98**, 135503 (2007).
- [10] C. P. Lusignan, T. H. Mourey, J. C. Wilson, and R. H. Colby, *Phys. Rev. E* **60**, 5657 (1999).
- [11] M. Daoud, *J. Phys. Lett. (France)* **40**, 201 (1979).
- [12] P. G. de Gennes, *J. Phys. Lett. (France)* **38**, 355 (1977).
- [13] Y. Liu and R. B. Pandey, *Phys. Rev. B* **55**, 8257 (1997).
- [14] L. Guo, R. H. Colby, C. P. Lusignan, and T. Whiteside, *Macromolecules* **36**, 10009 (2003).
- [15] S. B. Ross-Murphy, *Polym. Bull. (Berlin)* **58**, 119 (2007).
- [16] S. A. Newman, M. Cloitre, C. Allain, G. Forgacs, and D. Breyens, *Biopolymers* **41**, 337 (1997).
- [17] M. Djabourov, J. Leblond, and P. Papon, *J. Phys.* **49**, 319 (1988).
- [18] W. Brown, *Dynamic Light Scattering* (Clarendon, Oxford, 1993).
- [19] R. Pecora, *Dynamic Light Scattering* (Plenum, New York, 1985).

- [20] P. Stepanek, Z. Tuzar, P. Kadlec, and J. Kriz, *Macromolecules* **40**, 2165 (2007).
- [21] M. C. Blanco, D. Leisner, C. Vázquez, and M. A. López-Quintela, *Langmuir* **16**, 8585 (2000).
- [22] D. Leisner, M. C. Blanco, and A. López-Quintela, *Macromol. Symp.* **190**, 93 (2002).
- [23] M. Okamoto, T. Norisuye, and M. Shibayama, *Macromolecules* **34**, 8496 (2001).
- [24] T. Brand, S. Richter, and S. Berger, *J. Phys. Chem. B* **110**, 15853 (2006).
- [25] Y. Piñero Redondo, A. López-Quintela, and J. Rivas, *Colloids Surf., A* **270-271**, 205 (2005).
- [26] W. F. Harrington and N. V. Rao, *Biochemistry* **9**, 3714 (1970).
- [27] A. López Rodríguez and J. J. Freire, *Macromolecules* **24**, 3578 (1991).
- [28] P. Verdier and W. Stockmayer, *J. Chem. Phys.* **36**, 227 (1962).
- [29] K. Kremer, *Conference Proceedings on MC and Molecular Dynamics of Condensed Matter* (SIF, Bologna, 1996), Vol. 49.
- [30] A. López Rodríguez, J. J. Freire, and A. Horta, *J. Phys. Chem.* **96**, 3954 (1992).
- [31] A. Vegiri and C. Varsami, *J. Chem. Phys.* **120**, 7689 (2004).
- [32] P. J. Lu, E. Zaccarelli, F. Ciulla, A. B. Schofield, F. Sciortino, and D. A. Weitz, *Nature (London)* **453**, 499 (2008).